

Ductile fracture of thin shells and panels. Application to containment casings in aeroengines.

C Ruiz

University of Oxford
Department of Engineering Science
Parks Road
Oxford OX1 3PJ

Resumen. Se presenta un estudio sobre el valor de parámetros elastoplásticos de mecánica de fractura para el estudio de la iniciación de grietas en tuberías y estructuras de pared fina. Se demuestra que el ángulo de apertura de grieta (COA) es preferible a la integral J y al desplazamiento en fondo de grieta (CTOD). Se describe un método para decidir si la grieta se propaga rápidamente y el efecto de barreras como refuerzos y cambios de sección. El método requiere la medición del COA y un análisis por elementos finitos en el campo elastoplástico verificado experimentalmente.

Abstract. The relevance of elastoplastic fracture mechanics parameters for the study of crack initiation in pipelines and thin-walled structures is considered. It is shown that the crack opening angle (COA) has advantages over the J-integral and the crack tip opening displacement (CTOD). A methodology to find whether fast crack growth occurs and the effect of crack arresters such as raised flanges or changes in section is proposed. This relies on the measurement of the COA, a finite element elastoplastic analysis and experimental verification.

1. INTRODUCTION

The safety of gas pipelines has prompted much of the research into crack propagation in ductile materials. Early codes of practice [1] relied on engineering judgment based on experience. They attempted to ensure integrity by specifying materials with a Charpy V impact energy above a minimum value and geometrical defects in the pipeline within certain tolerances. Statistical analysis of full scale tests reproducing service conditions helped to draft rules that have proved remarkably effective. More recently, the emphasis shifted to the application of linear elastic fracture mechanics, in line with practice in the pressure vessel industry. It was argued that fracture initiation would be avoided by maintaining the calculated stress

intensity factors associated with permissible defects below the fracture toughness of the material, K_{IC} . While successful when dealing with the thick sections normally found in pressure vessels where the dominant failure mode is plane strain, this approach has been shown to be inappropriate to the predominantly plane stress conditions found in the ductile failure of pipelines. [2] In that case, elementary limit analysis has provided accurate predictions of the bursting pressure of pipelines with known defects. While an undoubtedly useful approach, limit analysis does not account for the deformation preceding failure and can not be applied to the study of propagating cracks.

Fast crack propagation has become an important consideration in the design of

containment casings for aero engines. In these most of the thrust is provided by the fan which consists of between 22 and 26 blades each weighing about 15 to 20 kg and turning at a peripheral tip speed of 400 to 475 m/s. These fan blades obviously have a large kinetic energy and the possibility that one may become detached cannot be ignored. Indeed, airworthiness regulations demand that a fan blade released at full power must be contained within the engine and a safe shut down can be effected without hazard to the aircraft. The casing structure must therefore be designed so as to allow the blade to move out of the path of the rest of the fan while preventing it from leaving the engine cowl. This is achieved by letting the blade perforate an inner membrane and containing it within an outer casing. It is essential to ensure that the perforation does not trigger the destruction of the inner casing that would result if extensive crack growth followed impact. [4]

There are other situations in the aero engine and airframe industries where crack growth

in stressed structures presents a serious threat: fracture of combustion chambers under a sudden overpressure and of a pressurised fuselage are two examples. [5,6] A number of features are common:-

1. The material is ductile and relatively large plastic structural deformation occurs during the failure process.
2. The structure is under static or quasistatic load prior to the event that triggers crack initiation.
3. External loads continue to be applied during crack growth.
4. Fracture is mainly in shear.

The role of plastic deformation, both at the stage of crack initiation and of crack growth, is regarded as the key to the whole process. In this report, some recent work will be surveyed and current practical procedures followed to avoid the problem will be briefly discussed.

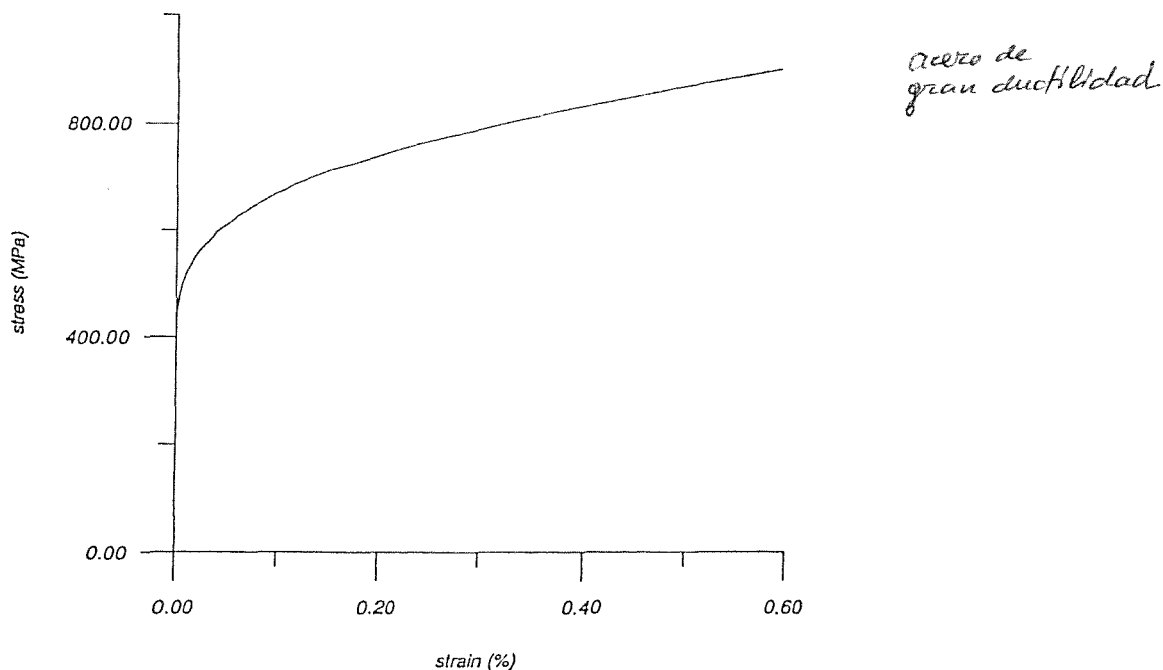


Figure 1. True stress-strain curve for gas pipeline steel [8]

2. PLASTIC INSTABILITY AND CONDITION FOR DUCTILE FRACTURE

Once the true stress - natural strain curve for the material is known, it is possible to find the bursting strength of a cylindrical pressure vessel or pipeline by means of the Considere's construction. [7] Taking, for example, a typical mild steel for gas pipelines whose mechanical properties are defined in figure 1, it can be shown that the bursting pressure due to plastic instability for a pipeline with nominal outside diameter $D = 914$ mm and nominal thickness $t = 15$ mm is 22.0 MPa. The bursting pressure can also be obtained by finite element analysis, plotting

the curve pressure viz. radial expansion for the pipeline with the material defined by figure 1. Using ABAQUS, it was found that the radial expansion tended to grow towards infinity when the pressure exceeded 21.86 MPa, in good agreement with the result obtained from the classical approach. [8] When a longitudinal crack of depth a is present, the strength of the pipeline should be reduced by the ligament efficiency factor, $(t-a)/t$, assuming that failure is still governed by plastic instability. In practice the material is not infinitely ductile and failure will occur through crack tearing at a lower pressure. As shown in Table 1, experimental results support this view.

Table 1
Calculated and experimentally determined bursting pressures [8]

Pipe No.	Outside diameter (mm)	Thickness (mm) t	Crack depth (mm)	Calculated* pressure (MPa)	Experimental pressure (MPa)
0	914	15	0	21.9 = p_{lim}	20
1	914	15	7.2	11.4	10.43
2	916.4	16.3	8.2	10.9	10.47
3	914.7	15.5	9.6	8.3	7.6

* Average of Considere's and ABAQUS results

Crack tearing may occur when a characterising parameter such as J , COD, etc. reaches a critical value. Using ABAQUS and the true stress-natural strain curve of figure 1 to represent the material, J and the crack opening displacements at the mouth and at the tip of the crack as well as the crack opening angle were calculated.

The physical meaning of the crack opening parameters is clear and unambiguous; the

crack tip opening displacement (CTOD) provides a measure of the plastic stretching which changes the sharp crack into a notch and the crack mouth opening displacement (CMOD) includes the change in flank angle, (COA).

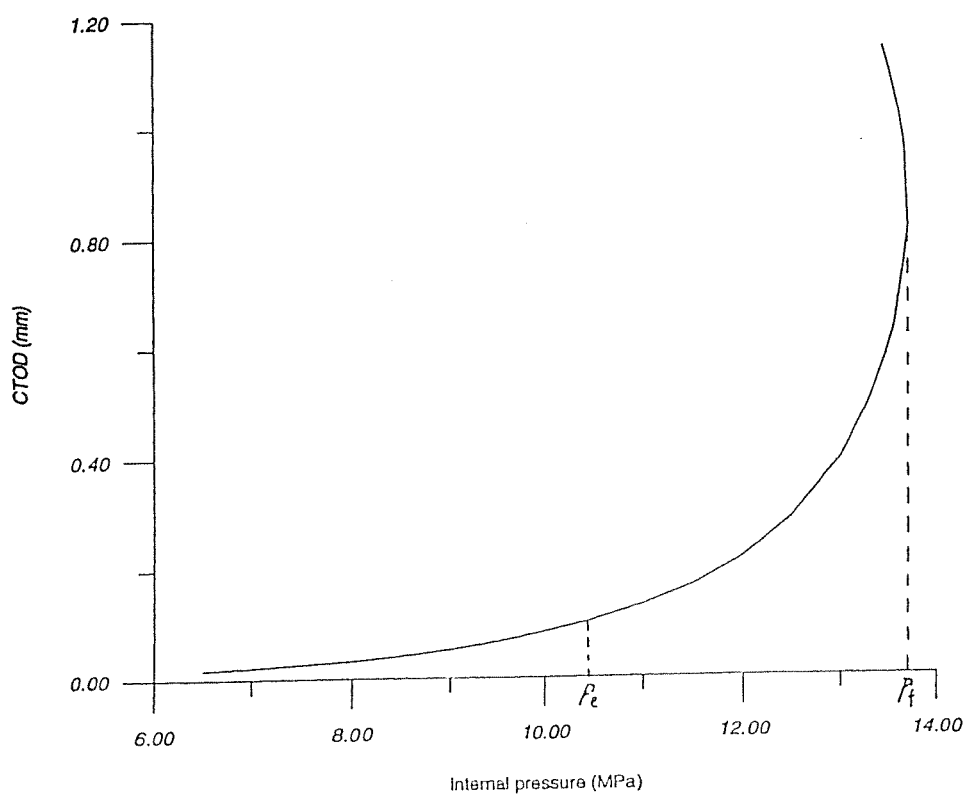


Figure 2. Relationship between internal pressure and CTOD for pipeline 1 [8]

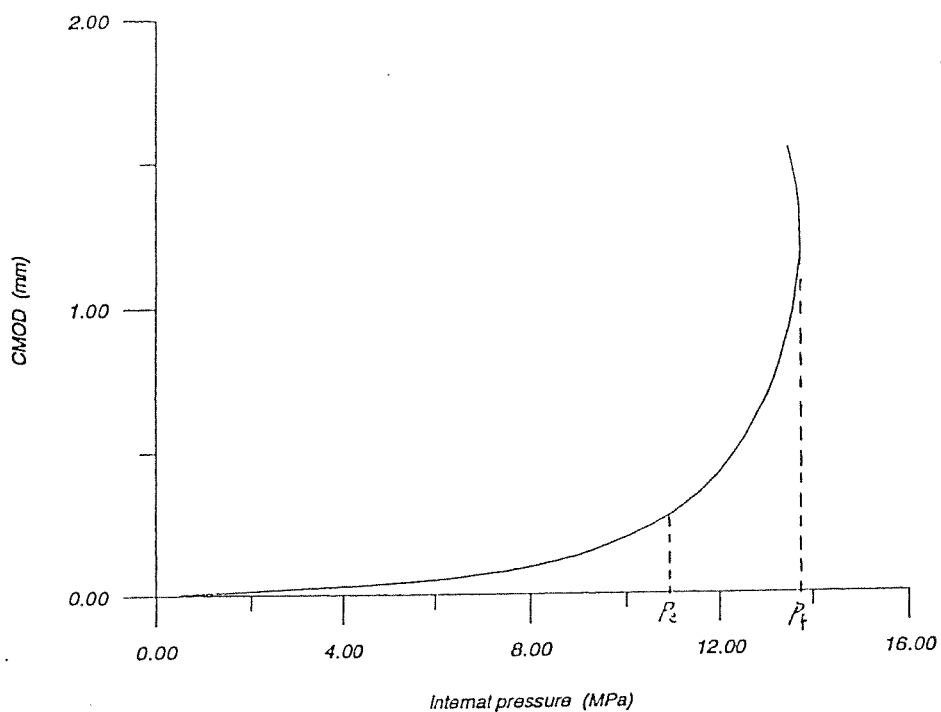


Figure 3. Relationship between internal pressure and CMOD for pipeline 1 [8]

Figures 2 and 3 show the variation of the CTOD and the CMOD with internal pressure for pipeline number 1. Similar curves were

obtained for the other pipelines. The values of the CTOD, CMOD and COA at bursting are shown in Table 2.

Table 2
Elastoplastic crack tearing parameters at the bursting pressure

Pipe No.	CTOD* (mm)	CMOD* (mm)	COA* (rad)	J (kJ/m ²)	P _r (MPa)
1	0.10	0.23	0.015	154	13.7
2	0.10	0.24	0.015	153	14.1
3	0.10	0.31	0.020	154	10.2

Note *: Values refer to one face of the crack only

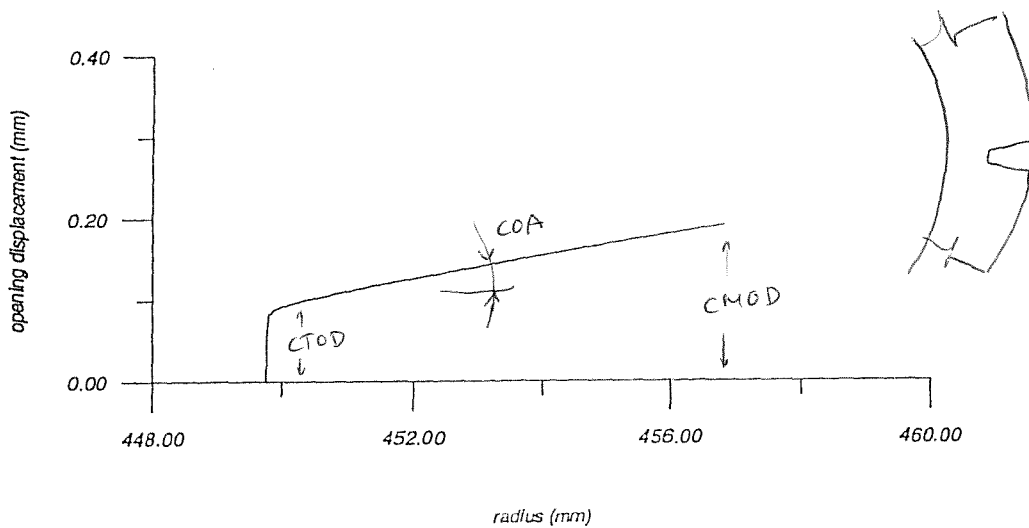


Figure 4. Crack opening shape for pipeline 1 at 10 MPa [8]

It will be noted that bursting occurs at a fixed value of the CTOD but that the values of the CMOD and of the COA differ by up to 19%. In all cases, as the pressure reaches a final value p_f , also shown in the tables, plastic instability would occur if the material were infinitely ductile. This final pressure exceeds the corresponding calculated and experimental values in Table 1. Figure 4 shows the crack profile at a pressure of 10 MPa. The flank is seen to remain straight. From a measurement of the CMOD and of the COA it is therefore possible to find the CTOD.

Although the physical meaning of J, as the strain energy released per unit of crack area, is perfectly clear, its calculation depends on finding a contour near to the crack tip but embracing an elastic region. Because of the widespread plastic deformation and the size of the crack it is very difficult to find a path independent value of J, as illustrated in figure 5. Contour number 1 is adjacent to crack tip, number 40 is at a distance of 5 mm. As the contour approaches the crack tip J decreases. Away from the crack tip there is a region over which it remains constant. The average values over this region, labelled AB in the figure, are given in Table 2.

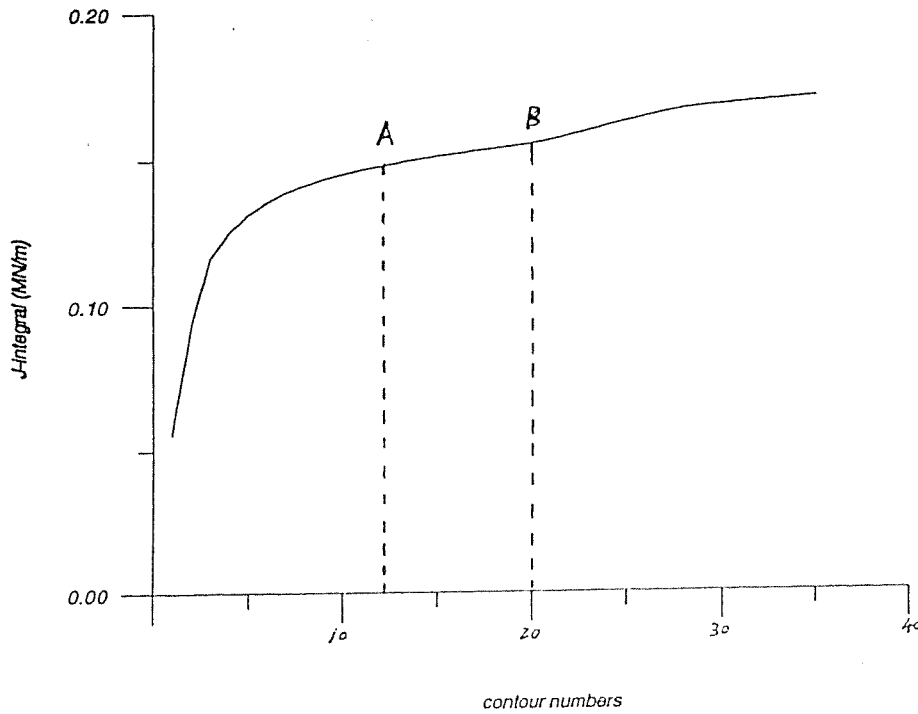


Figure 5. J - integral against contour numbers corresponding to experimental failure pressure for pipeline 1 [8]

Like the CTOD, J could be used to establish the critical condition for crack growth as a result of ductile tearing but, unlike the CTOD, it is not possible to measure J experimentally. This, added to the difficulty of calculating a path independent value of J precludes the use of J in practice.

3. CRACK PROPAGATION

The next question that arises is, what happens to the crack once the critical value of the CTOD has been reached? This problem has been studied by many researchers [5, 6, 9-12]. Where material toughness is high and in the case of thin-wall structures under plane stress conditions, failure occurs through plastic shearing. It

follows large displacements of the free edges behind the cracktip. The tear follows a route dictated by the orientation of the original defect and the state of stress of the structure until it is deflected by a change in wall thickness or material properties. Energy balance dictates that,

$$\text{Rate of work done by gas} = \text{Rates of elastic strain energy release} + \text{kinetic energy} + \text{plastic work} + \text{fracture energy} \quad (1)$$

The most important dissipative energy term is the rate of plastic work given the large deformation of the structure. Consider the pressurised cylindrical vessel or pipeline of figure 6.

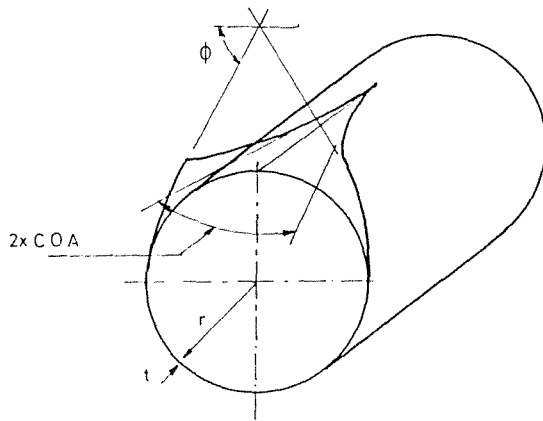


Figure 6. Ductile fracture of pressurised cylindrical vessel or pipeline

As the crack extends, it can be shown that the rate of elastic strain energy released is given by,

$$dU = - \frac{\pi r t \sigma^2}{E} da \quad (2a)$$

where σ is the initial stress, normally equal to two-thirds of the yield point.

The plastic work is associated with the opening angle of the pipe or vessel. For a rigid-ideally plastic material the rate of plastic work is given by

$$dW = \frac{1}{2} \phi \sigma_Y t^2 da \quad (2b)$$

where σ_Y is the yield point stress.

The fracture energy is,

$$dV = J t da \quad (2c)$$

and the rate of work done by the gas assuming adiabatic expansion as a first approximation,

$$dL = \frac{R\rho}{\gamma-1} T_2 \left[\left(\frac{P_2}{P_1} \right)^{\frac{\gamma-1}{\gamma}} \right] \pi r^2 da \quad (2d)$$

where the subindex 2 corresponds to the conditions prior to failure and p_1 may be taken to be equal to the atmospheric pressure. Other, more accurate, formulations of the rate of work done by the gas take into account the discharge flow rate but, for an order of magnitude assessment of the magnitudes involved equation (2d) is sufficient. Consider for example the case of a cylindrical pressure vessel with a radius of 1m, a thickness of 10 mm, made of steel with a yield stress of 450 MPa. The rate of elastic energy released (equation 2a) is 14.1 kJ/m; the rate of plastic work when the vessel opens by 180° is (equation 2b) 70.75 kJ/m, the fracture energy for $J = 150 \text{ kJ/m}^2$ is (equation 2c) 1.5 kJ/m. The overwhelming importance of the plastic work is clearly demonstrated. In contrast, the energy associated with crack tearing is virtually negligible. To give a design stress of 300 MPa, the gas pressure should be 30 bar. Assuming that the gas is air, with $R = 287 \text{ J/kgK}$, $\gamma = 1.4$ and a density of 1.225 kg/m^3 and that the temperature is 298 K, equation (2d) gives,

$$\frac{dL}{da} = 1350 \text{ kJ/m}$$

The vast disparity between the energy available and the energy required implies that the kinetic energy will be sufficient to project fragments of the vessel at very high velocities. This would not be the case if the pipeline contained a non volatile liquid. As another example, consider the containment casing of an aero engine made of an aluminium alloy, with a radius of 500 mm, a thickness of 2 mm, a yield stress of 300 MPa and $J = 80 \text{ kJ/m}^2$. From equations (2a) (2b) and (2c), the rates of elastic strain energy released, plastic work and fracture energy are found to be 1.8 kJ/m, 1.9 Jk/m and 0.16 kJ/m. Loading is due to its own weight and that of minor components supported by the shield and to the impact of the blade as it perforates the shield. While the fracture energy is again very small, the elastic energy released is almost equal to the dissipated plastic work. Only a small additional input of external energy would suffice to propagate the crack.

The conclusion that can be drawn from these examples is that the main terms in the energy balance equation, in addition to the external work, are the elastic strain energy and the plastic work, with any excess energy appearing as kinetic energy of the ejected fragments.

In consistency with this conclusion, a ductile fracture model has been proposed by Kanninen et al [13] for pipelines. The fundamental assumption is that the crack grows provided that the COA exceeds a critical value which is determined experimentally. An elastoplastic finite element is used to find the deformation of the pipeline as the crack grows and thus compare the calculated COA to the critical value. While the COA may not be ideal, as discussed in the previous section, it is much easier to calculate than the CTOD and it is also very easy to measure. It is however

expected that the CTOD would lead to more accurate predictions. There is no reason, other than practical considerations, why any elastoplastic finite element package should not be used once the external load is known. In the case of a pressurised gas container this is far from trivial since the pressure depends on the escaping gas flow through the opening whose size depends, in turn, on the pressure itself. Simple rules such as were used when deriving equation (2d) are not appropriate if an accurate solution is needed and the semiempirical equations proposed for gas pipelines [13] are clearly limited. There seems to be no other way than attempting to solve the coupled elastoplastic mechanics/gas dynamics equations by successive iterations, a tedious and expensive task. The problem is considerably eased if the loading is due to a non-volatile liquid under pressure or some other external force that remains constant or at least independent from the crack size as the crack grows.

4. IMPLEMENTATION OF THE MODEL FOR DUCTILE FRACTURE

The procedure for the implementation of the model for ductile fracture that has been described will be illustrated by an example taken from industrial practice. A containment casing for a large high by-pass ratio aero engine consists of an inner casing wrapped by several layers of woven Kevlar tapes. The inner casing is an aluminium alloy shell electrochemically machined to display reinforcing ribs on a hexagonal pattern, as in figure 7. The casing is fixed to a ring structure at one end and carries the intake cowl at the other. The stress level under normal operating conditions is approximately equal to one-third of yield and stresses in a containment incident do not raise over two-thirds of yield overall, although local plastic deformations will clearly be found close to the point of impact.

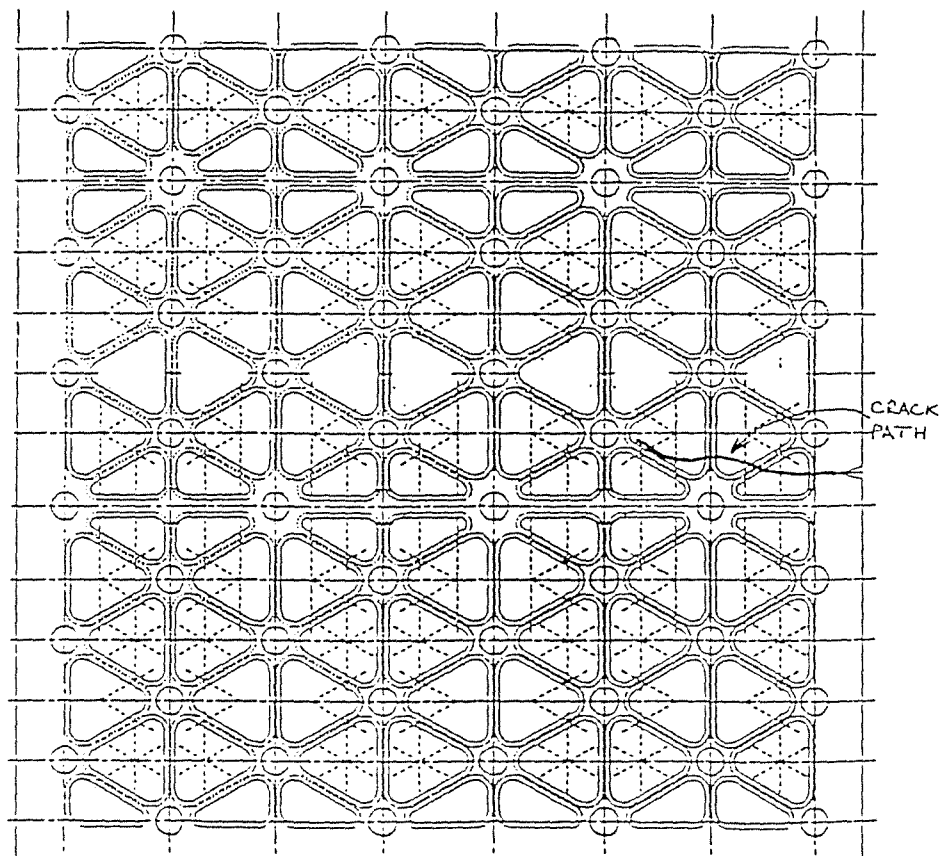


Figure 7. Typical Isogrid casing [15] Thickness of panels 2 mm, thickness of ribs 10 mm.

The shape and size of the initial defect, from which the crack starts, depends on the missile. This is a fan blade, normally hitting at the root end and forced against the casing by the other blades as they continue to rotate. Once the extent of this initial damage is established, the procedure is as follows:-

1. Calculate the COA of the damaged casing under the known external loads by means of ABAQUS [14]. If it is less than the critical COA, the crack will not grow. Note that the CTOD may be used instead.
2. If the COA calculated exceeds the critical value, the crack will grow. To find if it will accelerate, perform an energy balance as per equation (1), allowing the crack to extend over one of the cells of the isogrid.

3. If it is found that the crack accelerates, assume that its path is normal to the lines of maximum tensile stress and repeat the above calculations for various crack lengths.

The analysis requires an accurate material model in the form of true stress - natural strain relationship at the appropriate rate of strain and temperature and a critical value of the ductile fracture parameter COA, or CTOD. For the results to be accepted by the air transport licencing authorities they must also be verified preferably by a full-scale test but at least by means of some small-scale experiment designed to verify the fundamental assumptions made in the analysis.

4.1 MEASUREMENT OF CRITICAL DUCTILE FRACTURE PARAMETER

Recommendations for the measurement of the COA are found in [8]. Specimens, machined from actual pipelines, are tested in

3-point bending and the energy required to grow a crack from a pre-machined notch is found for two values of the notch depth. The value of the energy release rate is calculated by means of the following equation,

$$S_c = \left[\frac{U_1}{B(w-a_1)} - \frac{U_2}{B(w-a_2)} \right] \div [a_1 - a_2] = \left(\frac{\Delta U}{\Delta a} \right) \text{per unit area}$$

Defining the flow stress σ_F as,

$$\sigma_F = 0.65 (\text{Yield stress} + \text{Ultimate tensile strength})$$

the COA is obtained from the empirical equation,

$$COA = \frac{180}{\pi} \times 0.03086 \frac{S_c}{\sigma_F}$$

↑ ¡No son unidades consistentes!

All units are Imperial. See figure 8.

*Kanninen, Graut
Demafoni, Venzi*

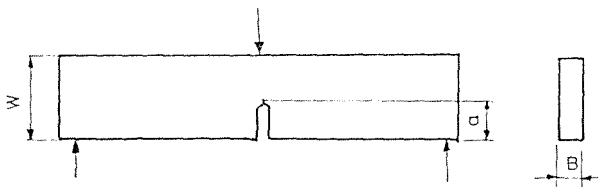


Figure 8. Three-point bend specimen for measurement of COA

A more rational procedure is based on the ASTM Standard for determination of crack arrest fracture toughness [16]. In this a compact tension specimen is fatigue precracked and the crack is opened by a wedge, as shown in figure 9. The crack

arrest fracture toughness, K_{Ia} , is given in function of the crack opening at the mouth by the equation,

$$K_{Ia} = E\delta f(x) \left(\frac{B}{B_N} \right)^{\frac{1}{2}} (W)^{-\frac{1}{2}}$$

where δ is the CMOD, which may be deduced from the displacement of the wedge B is the thickness, B_N is the thickness of the specimen along the fracture plane and W the width. $f(x)$ is a calibration function,

$$f(x) = 2.24 (1.72 - 0.9x + x^2) (1 - x)^{\frac{1}{2}} (9.85 - 0.17x + 11x^2)^{-1}$$

$$x = \frac{a}{W}$$

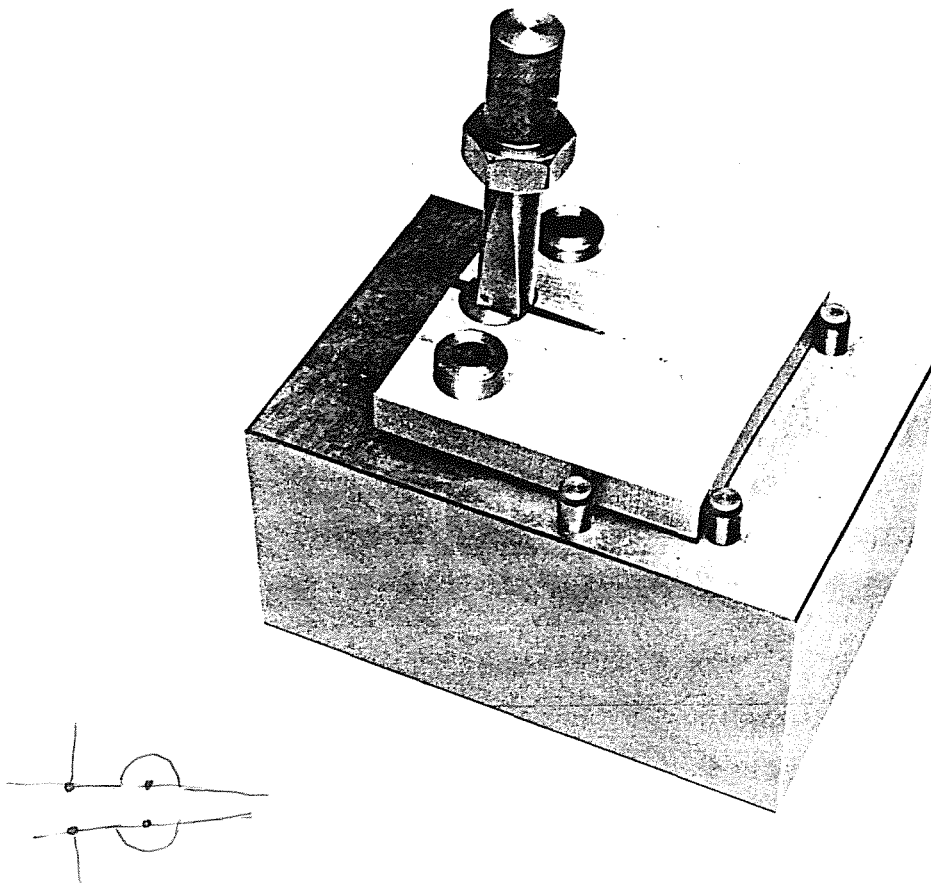


Figure 9. General arrangement for determination of crack arrest fracture toughness following ASTM guidelines

This test is meant to be used for fracture under plane strain conditions. The plane stress COA of the aluminium alloys used in the Isogrid has been measured directly with

the same testing procedure in Oxford. Two typical Al-Cu alloys with the following mechanical properties are of particular interest:-

Table 3
Properties of two typical Al-alloys

Alloy	Yield point (MPa)	Tensile Strength (MPa)	K_{IC} (MPa \sqrt{m})	COA (rad)
A	371	444	27.2	0.024
B	337	442	31	0.030

The relative difference between the two in fracture toughness is 13% and in COA it is 22%. It was found in practice that in casings made of alloy A cracks were much longer than in those made of alloy B.

4.2 VERIFICATION OF ANALYTICAL PROCEDURE.

To verify the accuracy of the predictions made following the analytical procedure that has been described it is necessary to monitor

the growth of a crack in a preloaded panel exhibiting those features of the real structure that are regarded as essential. A testing rig

designed and built for this purpose is shown in figure 10.

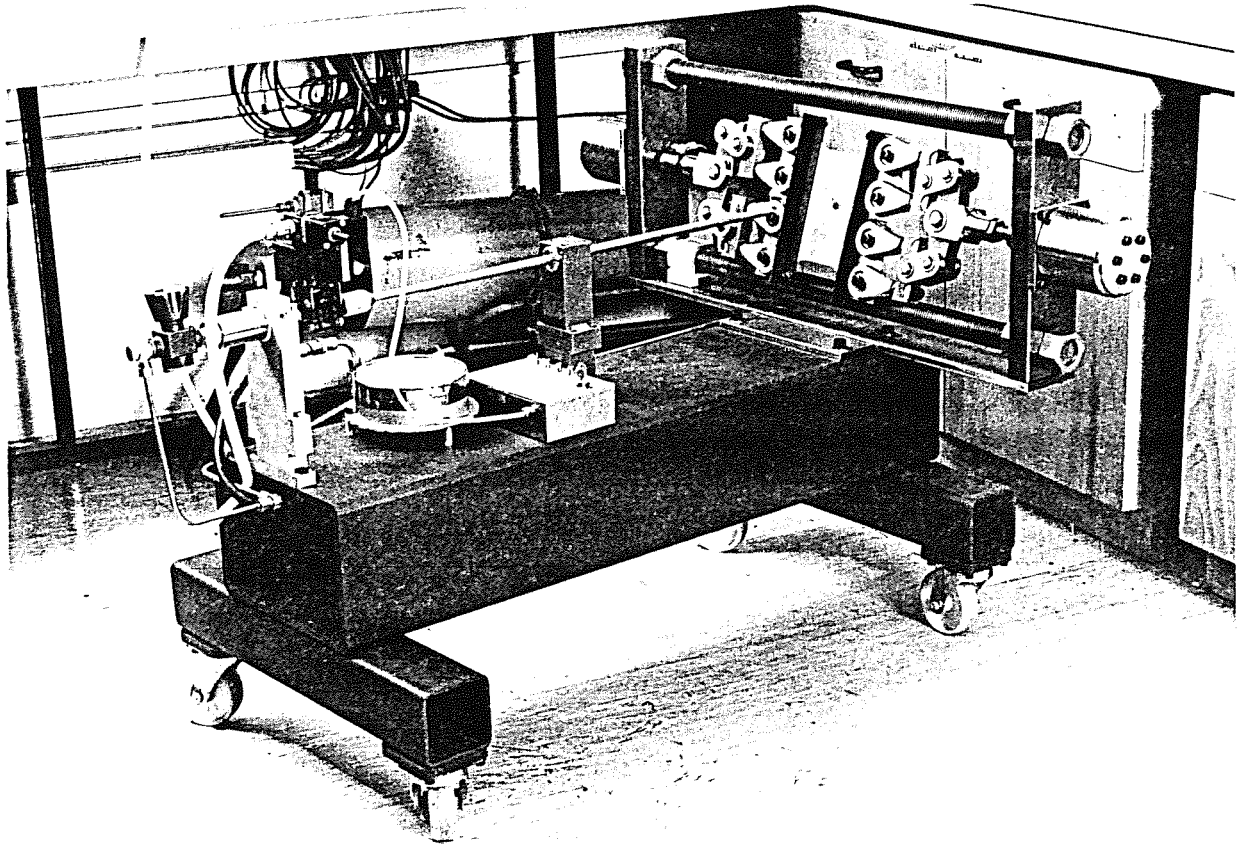


Figure 10. Test rig for the study of fast crack growth [17]

The specimen, in this case a plain panel 250 mm square is loaded by two identical pneumatic jacks capable of applying a load of 80 kN. Symmetry is important when dealing with phenomena involving stress waves and for this reason it was deemed preferable to have two jacks when one would suffice for static loading. By maintaining a large volume of compressed nitrogen as the pressurising fluid, the crack grows under constant force regardless of the

displacement of the clamps. It is also possible to achieve a fixed displacement condition by fitting collets to the loading stems. In the configuration shown in the figure, a projectile fired from a compressed gas gun perforates the specimen, causing the crack to initiate. Depending on the stress level in the panel the crack may arrest or cause the complete fracture of the panel. Features such as ribs, holes and changes of thickness may be included in the panel. A

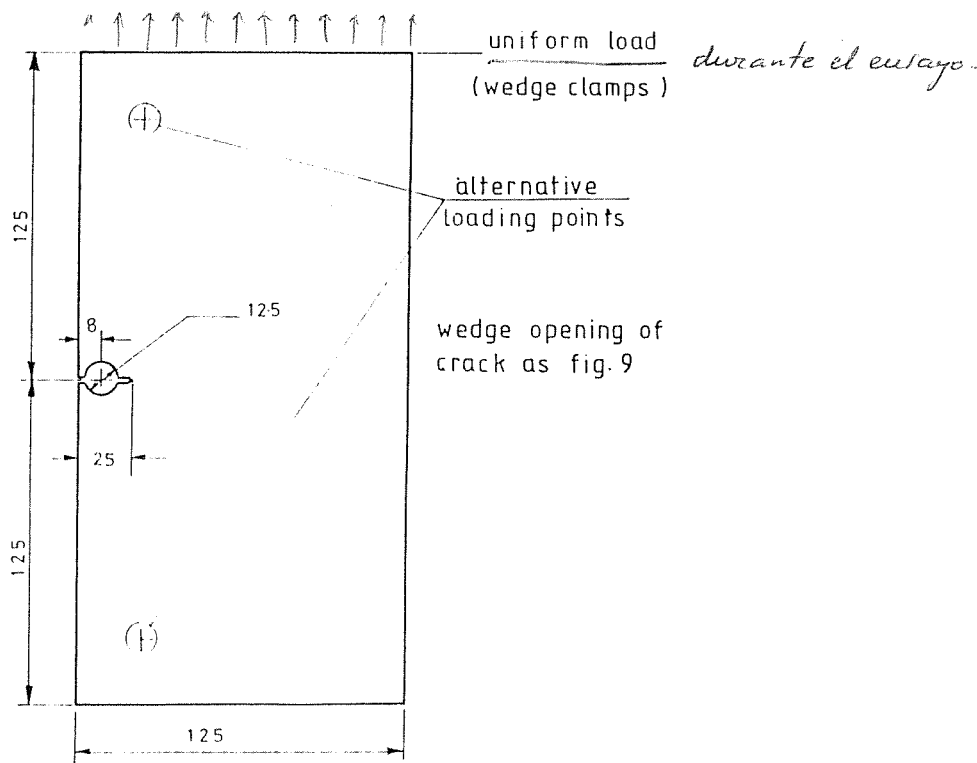


Figure 11. Test specimen for initiation of crack by wedge opening.

photodiode, located near the gun muzzle 'sees' the projectile and triggers an ultra high speed camera and a transient recorder to obtain the strain history at various points of the panel.

An alternative to this testing arrangement consists in combining the measurement of the COA and the verification of the analytical procedure. In this arrangement, figure 11, the notched specimen is loaded and the crack is initiated by hitting a wedge with a bar using an arrangement described in [18]. The transient recorder and photographic camera are triggered by a strain gauge fixed to the input bar. A clip gauge measures the CMOD and, from this, the COA can be deduced. Cracks grow under fixed force condition in a non-uniform stress field. As before, the

experiment provides data for the verification of the computer predictions.

5. CONCLUSIONS

A research programme to investigate the validity of the assumptions made in this paper and the accuracy of the results is currently under way in Oxford, supported by the EPSRC and by Rolls-Royce Aerospace. It is still too early to come up with any definite conclusions but it is already clear that a methodology based on elastoplastic fracture mechanics which considers only the energy associated with structural deformation, both elastic and plastic, external work and kinetic energy when the COA or the CTOD reach a critical value has considerable potential.

6. REFERENCES

1. British Gas, Inspection and repair of damaged steel pipelines, BGC/P5/P11, 1983
2. Corran, R.S.J., Davies, P.H. and Ruiz, C., Extremal elastic-ideally plastic solutions for assessment of flaws in notch-tough materials, Eng. Fract. Mech., 16, 1982, 585-604
3. Ruiz, C., Ductile growth of a longitudinal flaw in a cylindrical shell under internal pressure, Int. J. Mech. Sci. 20, 1978, 277-282
4. Ruiz, C. and Martindale, I.M., Containment of high energy fragments in aero engines, Seminar on Foreign Object Impact and Energy Absorbing Structures in Aerospace, I.Mech.E., London, March 1998
5. Kanninen, M.F., Marcharid, K.A. and O'Donoghue, P.E., Analysis of deformation and fracture of aircraft fuselages subjected to blast loading. FAA Workshop, Pleasantville N.J., April 1992.
6. Kanninen, M.F., Marchand, K.A. and O'Donoghue, P.E., An advanced fracture mechanics analysis of deformation and fracture in aircraft fuselages subjected to on-board blastloading, loc. cit. ref. 5.
7. Ruiz, C. and Koenigsberger, F., Design for Strength and Production., Macmillan, London, 1970
8. Tao, J. and Ruiz, C. Appraisal of methods of analysis of ductile failure, UTC Report No British Gas E24375, Oxford, Feb. 1996.
9. Kanninen, M.F., Grant, T.S., Demofoni, G. and Venzi, S. Development of theoretically based guidelines for the prevention of ductile fracture in gas transmission pipelines, Proc. PRC/EPRG 9th Tech. Meeting Line Pipe Research, Houston, May 1993.
10. Baum, M.R., Disruptive failure of pressure vessels, J. Pressure Vessel Techn., 110, 1988, 168-176.
11. Shoemaker, A.K. and McCartney, R.F., Displacement considerations for a ductile fracture in a line pipe, J. Eng. Materials, 95, 1974, 318-322.
12. Emery, A.F., Perl, M., Love, W.J. and Kobayashi, A.S., J. Pressure Vessel Techn., 103, 1981, 281-286
13. Kanninen, M.F., Grant, T.S. and Venzi, S. The development and validation of theoretical ductile fracture model, Proc. 8th Symp. on Gas Pipe Research, Houston, Sept. 1993.
14. ABAQUS, Users Manual, Version 5.6, Hibbitt Karlsson and Sorensen (UK) Ltd., Warrington, Cheshire, UK, 1997
15. Brooks, R., Rolls-Royce plc, private communication, July 1997.
16. ASTM, Standard Test Method for determining plane-strain crack arrest fracture toughness of ferritic steels, E1221-88, Annual book of ASTM standards, Vol. 03.01, 798-813.
17. Medina, J.L. and Ruiz, C., Fast crack growth in airframes and aeroengines. Preliminary Report. Rolls-Royce UTC for Solid Mechanics, Oxford, March 1998.
18. Corran, R.S.J., Benitez, F.G., Harding, J. and Ruiz, C., Towards the development of a dynamic fracture initiation test, Sih, G., Sommer, E. and Dahl, J., eds., Application of Fracture Mechanics to Materials and Structures, Nijthoff, 1984, 443-454